GLOBAL JOURNAL OF PURE AND APPLIED SCIENCES, VOL. 12 NO. 2, MARCH, 2006: 211-219
COPYRIGHT (C) BACHUDO SCIENCE COL. LTD. PRINTED IN NIGERIA, ISSN 1118-0579

DEVELOPMENT OF AN EXPERIMENTAL TEST-RIG FOR NATURAL GAS DIFFUSION FLAME STUDIES

J.C.OFODU and H.I.HART
(Received 7 February, 2005; Revision Accepted 25 July, 2005)

ABSTRACT

This work presents a part of a continuous research programme designed to provide information and experimental data leading to studies of soot and stable gaseous species from natural gas diffusion flame. This Test – Rig, which operates under atmospheric pressure, has along side with it a small probe (thermocouple attachment) for instantaneous measurement of temperature. The test rig has a co-annular burner consisting of a 16mm diameter steel tube (where the natural gas is injected upwardly) and surrounded by a 109mm diameter air annulus. The Rig and Facilities measures flame temperature, samples particulate matter (soot) and stable gaseous combustion product species within the flame with a well-designed Isokinetic sampling probe insert. After which, the natural gas species compositional change, soot volume fraction, soot number density can be determined with respect to axial and radial position distances from the burner rim.

KEYWORDS: Diffusion Flame, Temperature Profile and Isokinetic.

NOMENCLATURE

Re	Reynolds Number
v_{exit}	Exit velocity
d_{exit}	Burner exit diameter
Q	Volumetric flow rate
Z	Mixture fraction
Z_{st}	Stoichiometric mixture fraction
Φ	Equivalence ratio
Y_f	Mass fraction of fuel
a, b	Burner and oxidant flow path radius respectively
D	Mass Diffusivity
H, L	Flame Height

1.0 INTRODUCTION

The need to provide adequate and vast experimental data on the characteristics and structure of several diffusion flames, such as natural gas, is fast developing because of its necessity in the design of improved combustion systems. The readily needed flame characteristics include: heat release rate, gravimetric soot mass, stable gaseous emission species and compositional change of the fuel and its axial and radial distribution.

Soot and accompanied gaseous emissions of fossil fuel have a tremendous influence on the process efficiency of combustion systems. Soot is commonly, an undesired product of all combustion processes used for energy production (Jander *et al.* 1990; Bockhorn, 1994). It has been noted to increase the radiative heat loss that causes lower flame temperature, and affects the flow fields, which in turn reduces the efficiency of practical combustion devices. Soot and some gaseous species formation and propagation have a strong negative impact on the process kinetics and on the environment, including human health (some gaseous emissions are medically known to be caseinogens) (Lahaye *et al.* 1983; Bai *et al.* 1998).

Several methods exist for obtaining stable gaseous species concentration (CO, CO_2, NO_x) with respect to position of flame front. It could be moderately undertaken by the use of mass spectrometry or resonance – enhanced multiphoton ionization (REMPI) and Laser – induced fluorescence (LIF). The spatially resolved measurements of soot volume fraction (f_v), etc, can be carried out by the use of Laser scattering, Laser Induced Incandescence or Light Extinction Technique.

These aforementioned techniques sound good, but they are not available here in Nigeria (even if they are available, they are simply out of reach). Hence, to enhance research in this arena, and possibly determine the variation of gas composition in a nearly one – dimensional flame, a gravimetric method is used. Under this method, sample withdrawal technique is employed. It has been used in many studies to extract gas samples from flames; Gore and Zhan (1996), Friedman *et al* (1955), Choi *et al* (1994), and Choi *et al* (1995). Crookes et al (1996) described an experimental test rig (high pressure continuous liquid – fuel spray combustor) that can safely work at pressures up to 2.0 Mpa with overall input equivalence ratios in the range of 0.7 to 1.3. This installation was desired to measure particulate matter and gaseous combustion product species. Sunderland and Faeth (1996) designed adequate test rig for flame studies. Like wise Omer Gulder (1995) and Ian Kennedy et al (1996) researched extensively on this arena.

The primary focus of this paper is to present, step-by-step design and fabrication of an experimental test rig for studies of natural gas diffusion flame. This is highly important for Nigeria whose reservoir of natural gas is large enough to stimulate interest in the development of technologies that will ensure its large – scale utilization; this work is one of them, Ofodu (2004). Nigerian natural gas availability is estimated to be 120 trillion standard cubic feet (scf) of proven gas reserves, with 2 billion scf of

J.C.OFODU, Department of Mechanical Engineering, University of Port Harcourt, Nigeria
H.I.HART, Department of Mechanical Engineering, Rivers State University of Science & Technology, Nigeria

associated gas produced daily, 1.75 billion scf of it flared. Only about 12.5% is currently being used for commercial purposes. mainly for power generation and re-injection to enhance oil recovery, Federal Republic Nigeria (2000) and Ogbunbumi (2001). Results presented here are those of axial and radial temperature distribution for two test runs of equivalence ratios 0.35 and 0.90. This compares favourably with the works of Musick et al (1996) and Bernstein, et al (1993) both on methane flame studies.

2.0 DETAILED DESIGN

2.1 Velocity Range

The velocity of flow of fuel and oxidant (air) must be well harmonized such that the resulting combustion condition will be within laminar regime. Laminar combustion is marked by low Reynolds Number of (air and fuel flow) less than 2000. The Reynolds number based on the cold fuel and air gas properties at the fuel exit from the nozzle is hereby used;

$$Re = \frac{\rho v_{exit} d_{exit}}{\mu} \quad (1)$$

2.2 Mixture Fraction and Equivalent Ratio

A very important quantity or parameter for theory of diffusion combustion is the mixture fraction. Mixture fraction Z, as a quantity is the fuel atom mass fraction. It can be defined as the local mass fraction of all elements within the mixture originating from the fuel feed. Mathematically, it is popularly written as;

$$Z = \frac{m_1}{m_1 + m_2} \quad (2)$$

where m_1 = mass flux of fuel and m_2 = mass flux of oxidizer stream. Also, 1 – Z represents the mass fraction of the oxidizer stream which exists locally in the unburnt mixture. In terms of the fuel – air equivalent ratio (Φ).

$$\Phi = \frac{Z}{1-Z}\left(\frac{1-Z_{st}}{Z_{st}}\right) \quad (3)$$

Where: Z_{st} = Stoichiometric mixture fraction = $\left[1 + \frac{\nu Y_f}{Y_{0_2}}\right]$,

Y_f = mass fraction of fuel,
Y_{02} = mass fraction of oxygen, ν = stoichiometric oxidizer to fuel ratio.

2.3 Height of Flame and Boundary of the Flame Front

This analysis helps to predict the vertical height of the experimental test rig, most especially, the chamber set-aside for the flame visualization. The flame height or length H, is defined as the distance from the nozzle on the centerline of the flame to where the mean mixture fraction is equal to the stoichiometric value Z_{st}. In other words it should be seen here as the axial position at which the fuel is fully consumed. At this position most of the fuel is burnt and convection of hot gases is dominant at axial positions downstream. The value of the flame height is a function of velocity of flow of fuel, and the size of the fuel nozzle and that of the oxidizer stream.

To properly determine the flow configuration and flame contour of a vertical jet diffusion flame, the following parameters and values apply to this condition.
Burner internal diameter (D_{ngn}) = 16mm = 0.016m, with radius, a = 8 x 10^{-3}m.
Oxidant internal diameter (D_{an}) = 109mm = 0.109m, with radius, b = 5.45 x10^{-2}m.
Fuel exit velocities (V_{ng}) are = 0.042 and 0.084 m/sec., for equivalence ratios of 0.35 and 0.90 respectively. Oxidant maximum exit velocity (V_a) is maintained at a constant value of 0.0268 m/sec.

The flow configuration and flame contour of a vertical diffusion jet flame can be determined by applying the popular Burke – Schumann model. Methane, which is the predominant specie of the fuel/air diffusion flame, is used.

$CH_4 + 2(O_2 + 3.76N_2) \Rightarrow CO_2 + 2H_2O + 7.52N_2$

The stoichiometric mass or mixture fraction of fuel (Z_{st}) of methane CH_4 which is the predominant component of natural gas can be obtained, thus;

$$Z_{st} = \frac{16}{16 + (2\times 32) + (7.52\times 28)} = 0.0551$$

Also, F_s (stoichimetric fuel to air ratio) = $\frac{Z_{st}}{1-Z_{st}} = \frac{0.0551}{0.9449} = 0.0583$.

Thus, the solution of the Bessel function for Z_{st} = 0.0551 yields the location and size of the flame front for a given geometry of the combustion system. Defining an important factor, F, the ratio of mass flowrate of fuel to the mass flowrate of oxidant, we have;

$\frac{\rho V_{ng} A_{ng}}{\rho V_a A_a} \approx 0.593948134 V_{ng} = 0.0249,\ and\ 0.0499$ With the values of a and b being 8 x 10^{-3}m and 5.45 x 10^{-2}m, which stands for the radius of the burner and oxidant flow path respectively, we have F ≈ 0.0249, and 0.0499 for equivalence ratios of 0.35, and 0.90 respectively. For the fact that F< F_s, for equivalence ratios of 0.35 and 0.90, the resulting flame is over ventilated and this indicates a lean mixture. Had it been that F > F_s for equivalence ratios of the above, then, the resulting flame configuration would have been under-ventilated, indicating a rich mixture. Under-ventilated condition also indicates that the flame front will not terminate at the axis of symmetry for the geometry being considered.

2.4 Bessel Functions

From Burke-Schumann model, the general solution of Bessel function for this given condition can be stated as;

$$Z_{st} = \left(\frac{a}{b}\right)^2 + \frac{2a}{b}\sum_{j=1}^{\infty} \frac{J_1\left(C_j\frac{a}{b}\right)J_0\left(C_j\frac{a}{b}\right)}{C_j\left[J_0(C_j)\right]^2} \cdot \exp\left(\frac{-C_j^2 x}{Pe\, b}\right) + ..$$

Where Peclet Number Pe, is the ratio of convective flow to diffusive flow,

$Pe = \frac{V_{ng} b}{D}$, based on the fuel flow rate.

Mass Diffusivity D is given as;

$$D = 0.2\times 10^{-4}\left(\frac{T}{273}\right)^{1.69} m^2/s.$$

The above expression for diffusivity is for methane and air mixture. It is to be noted that, T will be used in this expression as 298 K. Also, J_0 and J_1 are Bessel functions of the first kind. C_j represents a family of positive roots of $J_1(C_j) = 0$. Values of $J_0(x)$ and $J_1(x)$ are tabulated for

different values of x from which the C_j's are obtained graphically as the x – values at which $J_0(x)$ and $J_1(x)$ are zero, respectively.

Expanding the solution of the Bessel function gives;

$$Z_{st} = \left(\frac{a}{b}\right)^2 + \frac{2a}{b}\left[\frac{J_1\left(C_1\frac{a}{b}\right)J_0\left(C_1\frac{a}{b}\right)}{C_1[J_0(C_1)]^2}\cdot\exp\left(\frac{-C_1^2x}{Pe\,b}\right)\right]_{j=1} +$$

$$\frac{2a}{b}\left[\frac{J_1\left(C_2\frac{a}{b}\right)J_0\left(C_2\frac{a}{b}\right)}{C_2[J_0(C_2)]^2}\cdot\exp\left(\frac{-C_2^2x}{Pe\,b}\right)\right]_{j=2} + \ldots\ldots\ldots$$

Observe that; C_j is the positive root of $J_1(C_j) = 0$.

Thus; $J_1\left(C_2\frac{a}{b}\right) = 0$, with $C_2\frac{a}{b} = C_1$. Then,

$$\frac{a}{b} = \frac{C_1}{C_2} = \frac{3.832}{7.016} = 0.5462$$

2.5 Solution Aimed at Determining The Flame Height

$C_1 = 3.832$; therefore, $\frac{2a}{b} = 0.2936$

$$C_1\frac{a}{b} = \left(3.832\times\frac{8\times10^{-3}}{5.45\times10^{-2}}\right) = 0.5625$$

$$\left(\frac{a}{b}\right)^2 = \left(\frac{8\times10^{-3}}{5.45\times10^{-2}}\right)^2 = 0.0215$$

$$Pe = \frac{V_{ng}b}{D} = \frac{0.042(5.45\times10^{-2})}{0.2\times10^{-4}\left(\frac{298}{273}\right)^{1.69}}$$

$$= 2349.935239V_{ng} = 98.697$$

And subsequently for equivalence ratio of 0.90, the Peclet number becomes 197.395. Hence;

$$\exp_1\left(\frac{269.44x}{Pe}\right) = e_1^{-2.730X} \text{ and } e_1^{-1.365X}$$

for equivalence ratios of 0.35 and 0.90.

Also, $\exp_2\left(\frac{903.197x}{Pe}\right) = e_2^{-9.151X}$ and $e_2^{-4.576X}$

$C_2 = 7.016$, and

$$C_2\frac{a}{b} = \left(7.016\times\frac{8\times10^{-3}}{5.45\times10^{-2}}\right) = 1.0299$$

$C_3 = 10.173$, and

$$C_3\frac{a}{b} = \left(10.173\times\frac{8\times10^{-3}}{5.45\times10^{-2}}\right) = 1.49$$

Applying to the solution equation, for equivalent ratio of 0.35 we have;

$$0.0551 = 0.0215 + 0.2936\left[\frac{J_1(0.5625)J_0\left(\frac{3.832r}{5.45\times10^{-2}}\right)}{3.832[J_0(3.832)]^2}\cdot e^{-2.730X}\right]_{j=1}$$

$$+ 0.2936\left[\frac{J_1(1.0299)J_0\left(\frac{7.016r}{5.45\times10^{-2}}\right)}{7.016[J_0(7.016)]^2}\cdot e^{-9.151X}\right]_{j=2} + \ldots\ldots\ldots$$

From table containing numerical values of Bessel function we have that;

$J_0(3.832) = -0.4025$, $J_1(0.5625) = 0.2423$

Also, $J_0(7.016) = 0.3001$, $J_1(1.0299) = 0.4401$

Hence,

$$0.0551 = 0.0215 + 0.2936\left[\frac{0.2423J_0(70.3r)}{3.832[-0.4025]^2}\cdot e^{-2.730X}\right]_{j=1}$$

$$+ 0.2936\left[\frac{0.4401J_0(129r)}{7.0160[0.3001]^2}\cdot e^{-9.151X}\right]_{j=2} + \ldots\ldots\ldots$$

This can be further reduced to;

$$0.0336 = 0.1146J_0(70.3r)e^{-2.730X}$$

$$+ 0.2045J_0(129r)e^{-9.151X} + \ldots\ldots\ldots$$

Since the flame is over-ventilated, then the flame front will terminate at the axis of symmetry (at a point x = L) where r = 0.

Therefore, at r = 0, $J_0(0) = 1$.

$$0.0336 = 0.1146e^{-2.730L} + 0.2045e^{-9.151XL} + \ldots\ldots\ldots$$

Let $e^{-x} = 1 - x$ to first order approximation,

Hence, $0.0336 = 0.1146[1 - 2.730L] + 0.2045[1 - 9.151L]$

With this arrangement, the height of flame H, or L becomes 0.131m = 13.1cm = 131mm. Subsequently, for equivalence ratio of 0.90 the theoretical flame height is hereby obtained to be: 26cm. Results of these along side with the visible measured flame height values for different equivalence ratios are graphically shown in figure 1. Higher accuracy would have been obtained if the expansion of the Bessel function were up to three terms.

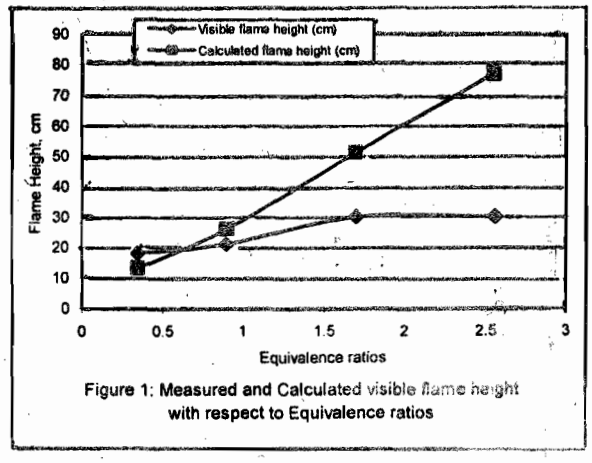

Figure 1: Measured and Calculated visible flame height with respect to Equivalence ratios

2.6 Flame Chamber and Casing

The most adequate material to be used for this item (flame enclosure) should have been a flexible steel mesh screen, but because of availability and cost, a galvanized sheet of 2mm thickness (16 gauge) is hereby used. This screen is designed to shield the flame from air movements in the laboratory. Also, there exists a window on one side of the casing made of tough 4.5mm thick glass material (melting point of 1414 ^{0}C), which provides optical access to the chamber for photographic shots (with a fast camera). It also provides access for personal visual inspection of the flame. The chamber casing, on one of the sides, has several provisional holes made for sample probe insert (isokinetically based).

To provide enough space for burner stand, height and mounting, the height of the chamber casing is

made to be 90 cm with square based width of 30cm. This item is secured to the base of the burner at the bottom, while its top is connected to a converging hopper - like unit that links through a needle-controlled valve.

2.7 Adiabatic Flame Temperature

In every combustion process, the chemical energy released is either lost as heat to the surroundings or used by the system to increase its temperature. This occurs if and only if the work interaction and changes in kinetic or potential energies are zero. With the application of the second law of thermodynamics, it is glaring that the smaller the heat loss, the larger the temperature rise. The maximum temperature of the products of the combustion attained by this condition of zero heat loss is termed the adiabatic flame or adiabatic combustion temperature of the reaction (T_f). After due computations, the value of T_f lies between 2300K and 2350K of which by interpolation, T_f = 2327.6K.

Caution

Stainless steel has a very high melting point. Hence, it is hereby adopted for the fabrication of the fuel nozzle and the burner.

2.8 Isokinetically Based Gas Sampling Probe Insert

Isokinetic sampling is the process of drawing a sample from a moving stream of gas at the same velocity as that of the free stream. This act is necessary because, if a sample is drawn at a velocity exceeding that of the free stream, a disproportionate amount of the smaller particles, being sampled will be drawn (converged) into the sampling nozzles, while the greater momentum of the larger particles would tend to carry them past. By the same token, if the sampling velocity is less than that of the free stream, a disproportionate amount of the smaller particles would tend to be deflected (diverged) past the nozzle. Thus, it is important to maintain a match between the free – stream velocity and the sample velocity.

To do this a number of requirements must be satisfied as follows;

- The user must ensure that the presence of sampling probe should not appreciably disturb the flow streamlines in the flame. The entrance of the probe must be sharpened to a knife – edge to prevent flow stagnation near the opening.
- Chemical reactions in the sampled gas must be suppressed immediately upon entry into the probe either with water or with air.
- An adequate method of gas analysis, such as the use of chromatography must be available.

Looking at these conditions, the requirements are contradictory, because flow disturbances would be minimized by an extremely small probe with very slow sample withdrawal, while on the other hand quenching would be facilitated by a completely water – cooled, and hence, relatively large probe. Also, for extremely slow sample – withdrawal, the choice of method for gas analysis becomes restricted to those applicable to very small samples. These contradictory requirements must be satisfied through proper design of this insert based on Isokinetic condition

Considerations: Consider the effluent gas flow into the chosen insertion probe in an attempt to justify the impossibility of disturbance to the flame streamline. Assume the unperturbed flow velocity of the hot flame gas is V_f. For Isokinetic condition to prevail one would expect this same value V_f to be obtainable in the probe. Let flow measurements under typical flame sampling conditions indicate that about Q_P flow rate (at flame temperature and pressure) of flame gas per second be drawn into the probe. Under this condition, one may compute the gas withdrawn for sampling to correspond to a flow across a

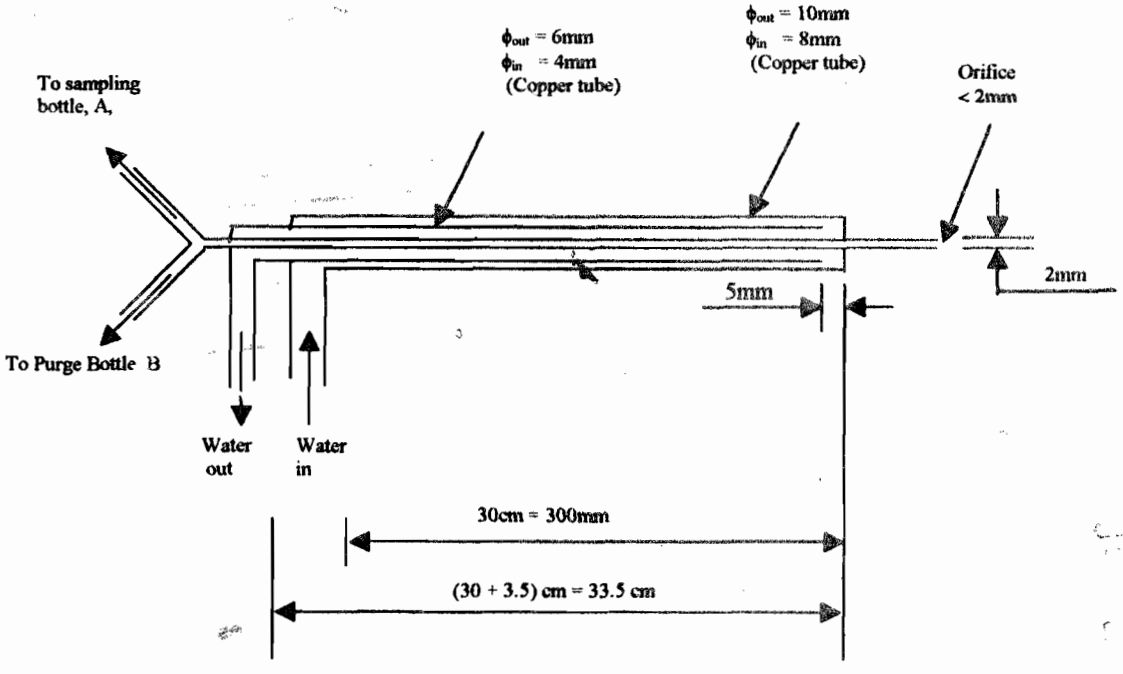

Figure 2: Isokinetic Probe Insert

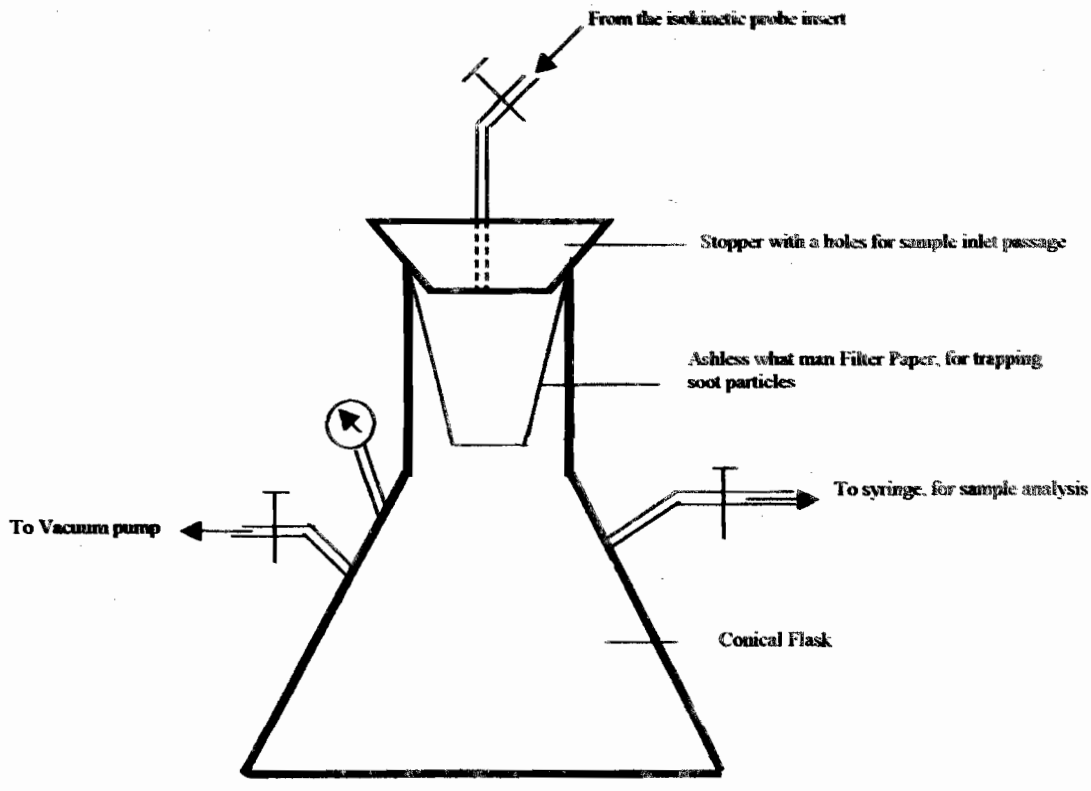

Figure 3: Sampling Bottle A

flame area of; $A_p = \frac{Q_p}{V_f}$. What this simple analysis entails is that, the diameter of the flow cross-section blocked by the probe tip must correspond to $d_t = \frac{4A_p}{\pi}$. When this is undertaken one would realize that flow disturbance due to sample withdrawal is small compared with disturbance due to probe size of the probe. After several computations based on trial and error it was found that the probe diameter should not be greater than 2.0mm. The diagrams, figure 2 and 3, show the arrangement of items including a Filter paper arrangement to trap in the soot particles (particulate matter of size 0.8). Alternatively, a Teflon Filter House can be incorporated or a polytetrafluoroethylene (PTFE) filter if need be. Owing to the expected flame temperature, the probe material used is stainless steel. But any other material whose melting point is within the range can serve.

2.8.1 Making of The Probe Insert Tip

Making the tip of probe orifice to be less than 2.0mm is extremely difficult as the necessary drawing equipment is not available, hence, this improvise method is hereby adopted. The probe is made of stainless steel pipe connected to two separate bottles A and B (sampling bottle and purge bottle respectively), figure 3. The sampling bottle contains a well-arranged Filter paper assembly to trap soot particles. The probe tip which is less than 2.0 mm is here achieved by inserting a tungsten wire of same size to the steel pipe inside diameter 2mm, outside diameter 3mm, constricting this end by a firm griping pliers such that removal of the tungsten wire by drawing will certainly leave a hole of same size which serves as the probe tip orifice. Note, that adequate distilled water is circulated to avoid formation of deposits in the narrow annular passages and to quench further reactions of soot as it traversed the length of the probe was connected within 5mm of the end of the probe. From recent literature, air-cooling is possible.

Caution: Should the orifice (probe tip) be clogged with soot deposits, which should occur occasionally and inevitably (substantial deposits of soot on the inner surface of the cold probe due to thermophoresis) the deposited soot has to be scrubbed from the probe and included in the determination of the total soot mass collected within the 2 minutes sampling period.

2.9 Optical and Access Window

A high tempered glass window (melting point of 1,414 ^{0}C) of dimension 40.2cm by 20.5cm (with edge rubber covering) was provided at one side of the test rig. This provides adequate optical access for visual observation and pictures of the flame. Figure 8, shows a schematic diagram of the arrangement of items of the Test-Rig.

Summary Of Design Dimensions
Chamber and Flame Casing
Size (Length and Width): 90cm x 30cm
Material: Galvanized Sheet

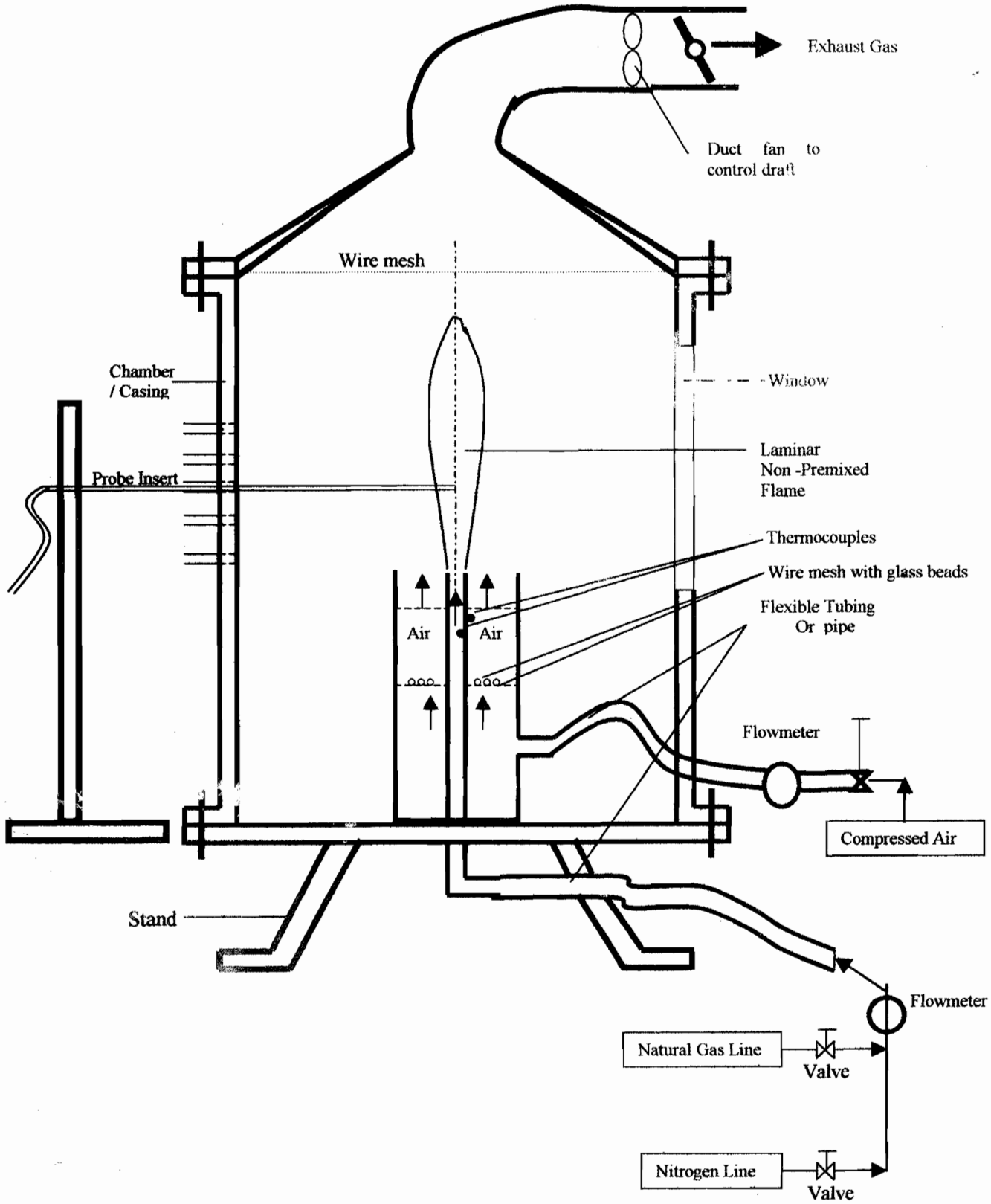

Figure 8: The arrangement of the entire Test-Rig

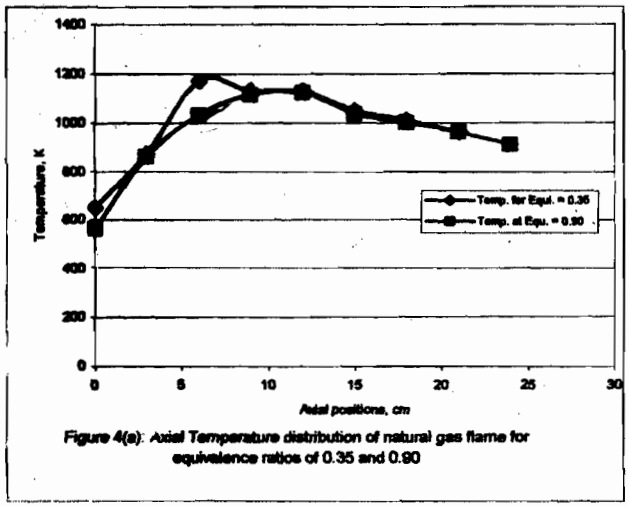

Figure 4(a): Axial Temperature distribution of natural gas flame for equivalence ratios of 0.35 and 0.90

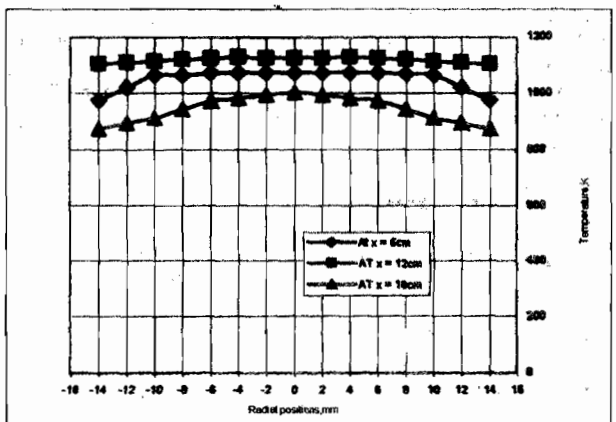

Figure 5(b): Radial Temperature plots for Equivalence ratio of 0.90 as obtained from the natural gas test rig

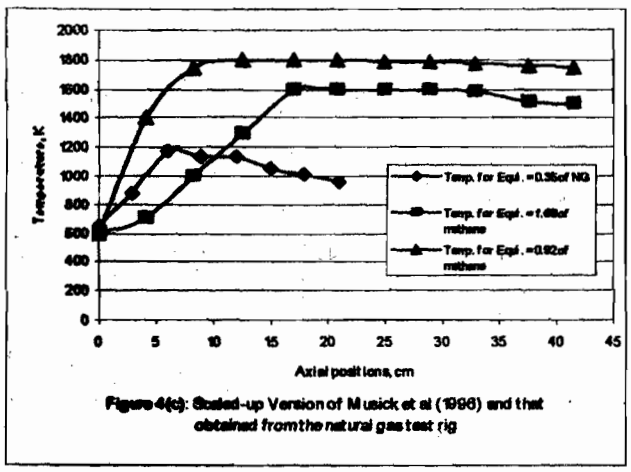

Figure 4(c): Scaled-up Version of Musick et al (1996) and that obtained from the natural gas test rig

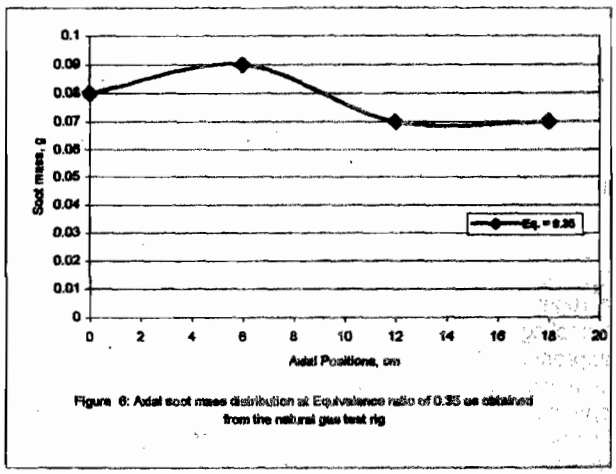

Figure 6: Axial soot mass distribution at Equivalence ratio of 0.35 as obtained from the natural gas test rig

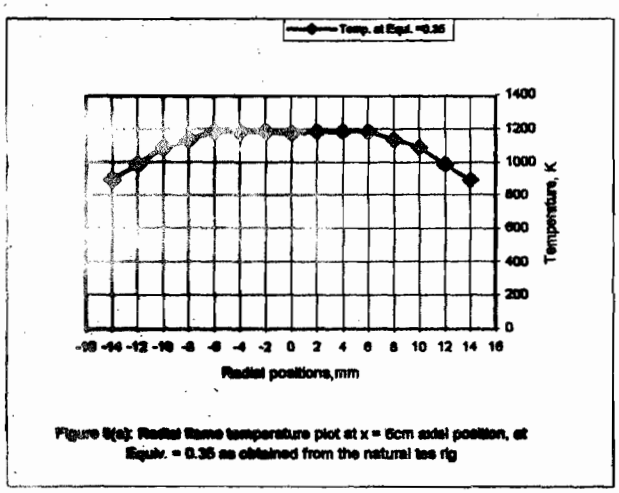

Figure 5(a): Radial flame temperature plot at x = 6cm axial position, at Equiv. = 0.35 as obtained from the natural tes rig

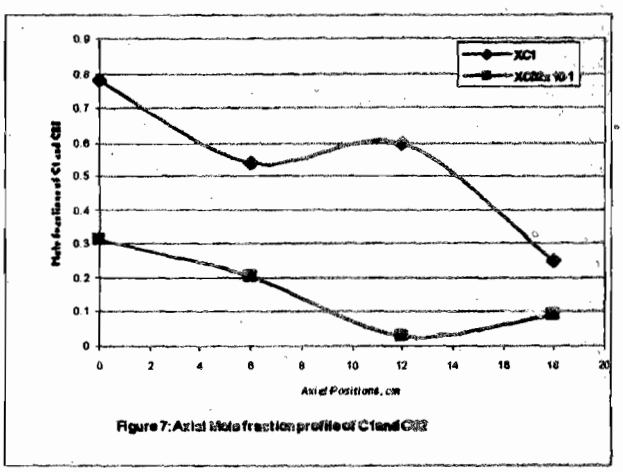

Figure 7: Axial Mole fraction profiles of C1 and C02

Fuel Nozzle
Size: 16.00mm = 0.016m, Inner diameter
Tube material: Stainless steel pipe
Length: 300mm = 0.3m
Area: 2.0×10^2 mm^2 = 2.0×10^{-4} m^2 = 0.0002m^2.

Burner Diameter (Air Nozzle)
Size: 109mm = 0.109m, Inner diameter
Tube material: Stainless steel pipe
Length: Less than 0.3m ≈ 0.25m
Area: 9.33×10^3 mm^2 = 9.33×10^{-3} m^2 = .00933m^2.

Sample Probe With Stand

Material: Stainless Steel, covered with two concentric cupper pipes
Size of Hole insert: 2mm opening

A k – type (Chromel - Alumel) thermocouple with well designed graduated attachment (error ± 0.01) which has been calibrated with Fluke 5502 Multi-product, Multi-

function calibrator, was used to measure axial and radial temperature profiles within the flame. The thermocouple was inserted through the sample pots (fifteen in number) made at the right hand side of the chamber. The temperature profile was measured for two different diffusion flames of equivalent ratios 0.35 and 0.90.

3.0 Experimental Procedure and Results

Having successfully designed and fabricated the experimental test rig, a natural gas-air diffusion flame of equivalence ratios 0.35 and 0.90 on a co-annular burner was established as a test run consecutively.

3.1 Temperature Profile Measurement:

3.2 Gaseous and Gravimetric Soot Mass, Within Diffusion Flame Measurement

The water – cooled sampling line has the arrangement shown in figures 2 and 3. To take a sample, the probe is moved quickly to the desired axial positions (0,3,6,9,12,15,18,21,24,27,30 cm) and/ or radial distance positions (0,4,8,12 mm).

There exist two sets of bottle; the sampling bottle A, (which should exist at a reduced pressure than 2atm) and the purge bottle B, (containing either helium or nitrogen existing at over – pressure for purge flow). Once the sample is to be taken, as the probe is being moved to the desired position, a small purge flow of helium or nitrogen should be allowed. Note that at this point, the sampling bottle is isolated. Once the probe is at the appropriate location, the purge flow valve is closed and the bulb isolation valve (leading to the sample bottle A) is opened. The sampling ends at about 2 minutes or immediately when the pressure in the sampling bottle reaches 1 atm. At this time, the bulb isolation valve (for sampling bulb) is closed and gas samples (approximately 10ml. Volume) are removed with a syringe for chromatographic analysis of the gaseous species, while the particulate matter is trapped by the funnel shaped filter paper. By careful removal of the filter paper from the conical flask and the cork after each run of the experiment it can be weighed to obtain the soot mass. Other parameters needed such as the soot number density, soot volume fraction, etc. can be computed from the appropriate relation.

3.3 RESULT AND DISCUSSIONS

Figure 1 shows the calculated and measured visible flame height in cm. The computed flame height was determined by applying the popular Burke-Schumann model. Detailed application of this concept to the various condition of flame as contained in this paper is available in section 2.5. The model predicted the flame height quite well at lean condition of flame (below the equivalence ratio of 1) while that at rich condition was over predicted.

The result of the temperature plots as obtained from this test rig in comparison with that obtained by Musick eta al (1996) is hereby presented (figures 4 and 5) with respect to axial and radial distances. The result presented in figure 4(a) as being obtained from the test rig is purely an enlarged version of that of Musick et al (1996) for methane with little variability. This is fairly good when the flame heights that resulted to these values are considered. For the natural gas flame, it is 18cm while that of methane was noted to be 1.0cm. Hence, with proper similarity adopted the results shown in figure 4(c) compare favourably.

Figure 4(a) shows the temperature profile measured at the flame axis starting from the burner exit point. The figure shows that the temperature rapidly rises from the cooler unburned core at the burner rim of about 600K to 1200K maximum value. Corresponding to approximately 6cm where it plateaus till 12cm from the burner rim. The rate of temperature increase within this region can be approximated to be 100K per distance, cm, from the burner exit. From this point, it falls gradually to the value of 1000K and fades away convectively.

Similarly, for equivalence ratio 0.90, the temperature profile as measured with the thermocouple along the vertical axis (axial) of the diffusion flame is shown in figure 4(a). The temperature just at the burner tip is slightly below 600K, non-significantly lower than that obtained by the flame of equivalent ratio 0.35. From this point, it grew axially to the maximum value of 1123K between 10 and 12cm position from the burner rim. This growth was at a reduced rate of 62K per unit axial distance compared to that of equivalent ratio 0.35. From this point, it reduces in value to 1003K precisely at 18cm from the burner rim and subsequently fades away convectively.

For the same condition of flame, equivalence ratio 0.35, a detailed temperature radial profile, at axial position of x = 6cm from the burner rim is shown in figure 5 (a) while that of equivalence ratio 0.90 at axial potions of x = 6, 12, 18cm are shown in figure 5(b). As expected, maximum temperature of 1200K which corresponds to that at axial distance of 6cm maintains this value to the outer stoichiometric flame zone (which marks the contour of the flame radially) at radial distance of 8mm from the burner rim. After this point, because of the high convective nature of the outer region the temperature decreases sharply to lower values.

Figure 6 shows the result of gravimetric soot mass (g). Along the centerline of the flame, soot mass of 0.08g was recorded at the burner rim after sampling for 120 seconds. It grows at a slow rate of 0.16% (corresponding to 0.0016 g per cm axial distance) measured along the flame centerline to a maximum value of 0.09g. From this point it continues to decrease and maintains a value of 0.07g till 18cm from the burner tip.

From figure 7, the concentration of carbon IV oxide (XCO2) decreases gradually in mole fraction from the value of 0.0312 at the burner rim to 0.0028 at about 12cm at the rate of 0.24% per cm distance. On reaching at the position of 18cm it increased to the value of 0.0093. Within these range of positions, the temperature behaved in a negative manner, that is, increasing whenever CO2 is decreasing and subsequently decreasing whenever CO2 is increasing. Also, figure 7 shows the graphical plot of the

mole fraction of C1 with respect to centerline distance within the flame. It is very ease to observe that for all the positions considered (1, 6, 12, and 18cm), that C1 decrease from the values of 0.781 (at the burner rim) to 0.5419 (at axial position of 6cm) and subsequently increased to 0.5979 (at axial position of 12cm) and finally decreased to a position of 18cm where it is believed to be fully consumed.

CONCLUSION

An experimental test rig for natural gas diffusion flame studies has been designed and fabricated. The rig has been tested and the following parameters measured: temperature, soot mass, visible flame height and gaseous species compositional change along the axis and radial distances of an over-ventilated flame of equivalence ratios 0.35 and 0.90. The results obtained compared favourably with previous work for methane fuel and this indicates an efficient rig design.

ACKNOWLEDGEMENT

The authors, acknowledge the help and valuable discussion and inputs made by Engr. Dr. D.P.S Abam, Department of Mechanical Engineering, University of Port Harcourt. The overwhelming support and assistance provided by Dr. Michael Balthasar, University of Cambridge, Prof. Fabian Mauss, Department of Combustion Physics, Lund Institute, Sweden. Recent relevant combustion papers received from Prof. Ian, Kennedy of University of California are all well acknowledged.

REFERENCES

Bai, X.S., Balthasar, M., Mauss, F. and Fuchs, L., 1998. Detailed Soot Modeling in Turbulent Jet Diffusion Flames, Twenty-Seventh Symposium (International) on Combustion, The Combustion Institute, Pittsburgh, pp. 1623 – 1630.

Bernstein J.S, Fein Asa, Choi J.B, Cool T.A, Sausa, R.C, Howard S.L, Locke R.J, Miziolek A.W., 1993. Laser – Based Flame Species Profile Measurements: A Comparison With Flame Model Predictions, Combustion and Flame, The Journal of Combustion Institute, Elsevier, America, 92(1): & (2): 85 - 105.

Bockhorn, H., 1994. *Soot Formation in Combustion Mechanisms and Models*, Springer Verlag, Berlin-Heidelberg.

Choi M.Y, Hamins A, Mulholland, G.W and Kashiwagi T., 1994. Simultaneous Optical Measurement of Soot Volume Fraction and Temperature in Premixed Flames. Combustion and Flame. The Journal of the combustion Institute, Elsevier, America, 99, (1): 174 – 186.

Choi M.Y, Hamins A, Mulholland G.W, HAMINS A and Kashiwagi T., 1995. Comparisons of the Soot Volume Fraction Using Gravimetric and Light Extinction Techniques. Combustion and Flame, The Journal of the Combustion Institute, Elsevier, America, 102 (½):161 – 169.

Crookes R.J, Kiannejad F, Sivalingam G, and Nazha M.A.A., 1996. Measurement of Soot – particle Emission Using a High-Pressure Continuous spray-Combustion facility. *Archivum Combustionis*, 16, (1): - (2): 23 – 35.

Federal Republic Nigeria, 2000; Report of the special committee on the review of petroleum products, supply and distribution. Federal Ministry of Information and National Orientation, Abuja, Nigeria.

Friedman, R and Cyphers, J.A, 1955. Flame Structure Studies III, Gas Sampling In a Low – Pressure Propane – Air Flame. Journal of Chemical Physics, 23(10): 1875 – 1880.

Gore J.P and Zhan N.J., 1996. Nox Emission and Major Species Concentrations in partially Premixed Laminar Methane/Air Co-flow Flames, Combustion and Flame, The Journal of Combustion Institute, Elsevier, America,105(3): 414 – 427.

Jander, H. and Wagner, H.G., 1990. Soot Formation in Combustion - An International Round Table Discussion, Vandenhoeck and Ruprecht, Gottingen.

Kennedy Ian M, Clement Yam, Darrell C. Rapp, and Robert J.Santoro, 1996. Modeling and Measurements of Soot and Species in a Laminar Diffusion Flame. Combustion and Flame, The Journal of the Combustion Institute, Elsevier, America, 107(4): 368 – 382.

Lahaye, J. and Prado, G., 1983. Soot in Combustion Systems and its Toxic Properties, Plenum Press, New York.

Musick, M, Van Tiggelen, P.J and Vandooren, J., 1996 Experimental Study of the Structure of several Fuel-Rich Premixed Flames of Methane, Oxygen and Argon. Combustion and Flame, The Journal of the Combustion Institute, Elsevier, America,.105: 433 – 450.

Ofodu, J.C., 2004. Experimental Study of Soot and Gaseous Emission In a Natural Gas Diffusion Flame, Unpublished Ph.D Write-Up, Department of Mechanical Engineering, Rivers State University of Science and Technology, Pp (1-215)

Ogbunbumi K., 2001. A long history of Oil Production Inefficiency. The Guardian, (March 25), 19: Nigeria.

Omer L. Gulder, 1995. Effects of Oxygen on Soot Formation in Methane, Propane, and n-Butane Diffusion Flames, Combustion and Flame, The Journal of the Combustion Institute, Elsevier.101 (3): 302 – 310.

Sunder Land P.B and Faeth G.M., 1996. Soot Formation In Hydrocarbon/Air Laminar Jet Diffusion Flames, Combustion and Flame, The Journal of the Combustion Institute, Elsevier, America,105,(½,): 132 – 146.